Correspondence

Adaptive Median Filters: New Algorithms and Results

H. Hwang and R. A. Haddad

Abstract—**Based on two types of image models corrupted by impulse noise, we propose two new algorithms for adaptive median filters. These have variable window size for removal of impulses while preserving sharpness. The first one, called the *ranked-order based adaptive median filter* (RAMF), is based on a test for the presence of impulses in the center pixel itself followed by the test for the presence of residual impulses in the median filter output. The second one, called the *impulse size based adaptive median filter* (SAMF), is based on the detection of the size of the impulse noise.**

It is shown that the RAMF is superior to the nonlinear mean L_p filter in removing positive and negative impulses while simultaneously preserving sharpness; the SAMF is superior to Lin's adaptive scheme because it is simpler and better performing in removing the high density of impulsive noise as well as nonimpulsive noise and in preserving fine details. Simulations on standard images confirm that these algorithms are superior to standard median filters.

I. Introduction

In image processing, images are often corrupted by positive and negative impulses stemming from decoding errors or noisy channels. Both are easily detected by the eye and degrade the image quality. The nonlinear mean filter [2], [3] cannot remove such positive and negative impulses simultaneously. The median filter performs quite well, but it falters when the probability of impulse noise occurrence becomes high. To overcome this situation, we propose a new algorithm for adaptive median filters with variable window size. This filter is to be robust in removing mixed impulses with high probability of occurrence while preserving sharpness. This algorithm, called the *ranked-order based adaptive median filter* (RAMF), is based on a two-level test. The first level tests for the presence of residual impulses in the median filter output, and the second level tests whether the center pixel itself is corrupted by an impulse or not.

In some image applications, it is frequently desirable to remove noise that might be impulsive and/or nonimpulsive, with minimum distortion of the original image information. One of the undesirable properties of the median filter is that it does not provide sufficient smoothing of nonimpulsive noise. To overcome this, various techniques [1], [4] have been used.

Recently, Lin and Wilson [5] proposed the median filter with an adaptive length based on impulse noise detection. As mentioned in [5], the 1–D scheme performs poorly for mixed impulse noise. A negative impulse noise can be incorrectly detected as positive impulse noise. They proposed the 2–D algorithms. For removal of such noise, one of them is to remove positive impulse noise and then remove negative impulse noise. Another one is to remove positive and negative impulse noise simultaneously. Because of high probability of false alarm in high density noise, the separate removal of positive and negative impulse noise was preferred. However, for such an algorithm, the false alarm described in the 1–D case still exists, and the operation becomes complex. In order to overcome these problems, we propose another new algorithm for adaptive median filters as an extension of Lin's adaptive scheme [5]. Our filter is simpler and better performing in removing a high density of mixed impulsive noise as well as nonimpulsive noise while preserving fine details. This algorithm, called the *impulse size based adaptive median filter* (SAMF), is based on detecting the size of the impulse and then adjusting the window length of the median filter.

In this correspondence, we have proposed two new algorithms for adaptive median filters. Our simulations on standard test images demonstrate that these filters are simpler and better performing than rival algorithms.

Manuscript received March 18, 1992; revised January 16, 1994. The associate editor coordinating the review of this paper and approving it for publication was Prof. Roland T. Chin.

H. Hwang is with the A/V R&D Center, Samsung Electronics, Suwon City, Korea.

R. A. Haddad is with the Department of Electrical Engineering, Polytechnic University, Hawthorne, NY 10532.

IEEE Log Number 9409286.

II. First Noise Model: RAMF

A. Noise Model

In the first case, we assume that each pixel at (i, j) is corrupted by an impulse with probability p independent of whether other pixels are corrupted or not. The impulse corrupted pixel e_{ij} takes on the minimum pixel value s_{min} with probability q_e or the maximum pixel value s_{max} with probability $1 - q_e$, when the original pixel s_{ij} is corrupted by a negative or a positive impulse, respectively. Let $\{x_{ij}\}$ be the noise corrupted image. Then

$$x_{ij} = \begin{cases} e_{ij} & \text{with } p \\ s_{ij} & \text{with } 1-p. \end{cases}$$

The RAMF algorithm is based on a test for the presence of an impulse at the center pixel followed by a test for the detection of a residual impulse in the median filter output.

B. Two-Level Filter Structure

In the first noise model, the nonlinear mean filters [2] fail to remove impulses whenever negative impulses are present; the standard median filters falter when p is large. The following analysis shows the ineffectiveness of the median filter in removing a high degree of impulse noise. We consider the special case $s_{ij} = 0$ inside the window W. In this case

$$x_{ij} = \begin{cases} e_{ij} & \text{with } p \\ s_{ij} = 0 & \text{with } 1-p \end{cases} \tag{1}$$

and e_{ij} is either $s_{min} = 0$ or s_{max}. Let x_{med} denote the median filter output

$$x_{med} = \text{med}\{x_{i+r,j+s}\}, (r, s) \in W. \tag{2}$$

Let N_{ij} denote the number of impulse-corrupted pixels in W centered at (i, j). It is shown in [6] that

$$E\{x_{med} | x_{med} = e_{ij}\} = \frac{E\{x_{med}\}}{1 - Pr[x_{med} = s_{ij}]} \tag{3}$$

where $Pr[x_{med} = s_{ij}] = Pr[N_{ij} \leq (W - 1)/2]$ is given in (C.1) in [6]. Note that (3) is a measure of the impulse-removal performance of the filter. Our objective is to improve on the fixed median by adaptively varying the window size, thereby reducing the error measure (3).

TABLE I
FIRST-LEVEL TRUTH TABLE; $\oplus$ IS THE EXCLUSIVE-OR OPERATOR, AND THE OVER BAR IS THE SET COMPLEMENT.

case	T_-	T_+	true hypothesis
(a)	0	0	$H_1\overline{H}_2\overline{H}_3 + \overline{H}_1H_2\overline{H}_3 + \overline{H}_1\overline{H}_2H_3$
(b)	0	negative	$H_1 \oplus H_3$
(c)	positive	0	$H_2 \oplus H_3$
(d)	positive	negative	H_3

TABLE II
SECOND-LEVEL TRUTH TABLE; $+$ IS THE EXCLUSIVE-OR OPERATOR.

case	U_-	U_+	true hypothesis
(a)	0	0	impossible
(b)	0	negative	$E_1 \oplus E_3$
(c)	positive	0	$E_2 \oplus E_3$
(d)	positive	negative	E_3

The RAMF consists of two levels. The first level tests for the presence of residual impulses in the median filter output. If the first level asserts there is no impulse in the median filter output, then the second level tests whether the center pixel itself is corrupted by an impulse or not. If the center pixel is decided as uncorrupted, then we leave it as is without filtering. If not, the output of RAMF is replaced by the median filter output at the first level. On the other hand, if the first level asserts there is an impulse in the median filter output, then we simply increase the window size for the median filter and repeat the first-level test.

Note that there is a loop in the first level. A termination condition for this loop is related to the impulsive noise density p. In our simulations, we found that a maximum window width $W = 5$ is adequate for $p = 0.3$, while $W = 11$ was needed for a large noise density corresponding to $p = 0.7$.

In the first level, the median filter output x_{med} can be cast into three possible disjoint values

$$x_{med} = \begin{cases} s_{min} \\ \tilde{s}_{ij} \\ s_{max} \end{cases} \tag{4}$$

where $\tilde{s}_{ij}$ is one of the uncorrupted pixel values, which range between s_{min} and s_{max}.

The specific values of s_{min}, s_{max} are not needed explicitly in the hypothesis test to follow. It is also pointed out that the uncorrupted pixel value $\tilde{s}_{ij}$ itself can take on these extreme values. So we cannot simply declare an impulse of noise present whenever $x_{med} = s_{max}$ or s_{min}. Hence, we need the more sophisticated hypothesis test described next.

Level I-RAMF: We define two test statistics T_- and T_+

$$T_- \triangleq x_{med} - x_{min} \text{ and } T_+ \triangleq x_{med} - x_{max} \tag{5}$$

where $x_{min}(x_{max})$ denotes the minimum (maximum) value inside the window. With three possible disjoint values for x_{med}, we define three hypotheses

$$H_1 : x_{med} = s_{min}, H_2 : x_{med} = s_{max}, \text{ and } H_3 : x_{med} = \tilde{s}_{ij}.$$

The truth table for these statistics is shown in Table I. In case d), we proceed to the second level. In cases a), b), and c), we increase the window size and repeat the first level. As mentioned earlier, we come out of the loop either by satisfying the test condition or by effectively terminating the looping through a choice of maximum window width W. At this point, the output of the first level is free of impulses so long as the test condition is satisfied.

Level II-RAMF: For the second level, we define the test statistics U_- and U_+ as

$$U_- \triangleq x_{ij} - x_{min} \text{ and } U_+ \triangleq x_{ij} - x_{max}. \tag{6}$$

The hypotheses over a region inside the window are denoted by

$$E_1 : x_{ij} = s_{min}, E_2 : x_{ij} = s_{max}, \text{ and} E_3 : x_{ij} = s_{ij}.$$

The truth table for these statistics is shown in Table II. If d), then the RAMF output is the center pixel itself; otherwise, the RAMF output is the x_{med} of the first level.

C. Simulation Results

The RAMF filter is used on the standard test image, as shown in Fig. 1(a), of 8 bits per pixel. Fig. 1(b) shows the corrupted image by mixed impulses with $p = 0.3$ and $q_r = 0.5$ in the first model. Fig. 1(c) shows the RAMF filtered image with a maximum 5×5 square-shaped window. For comparison, the nonlinear mean L_p filter [2] and the median filter are applied to the same input image. Fig. 1(d) shows the L_p (with parameter $p = 3$) filtered image with negative impulses removed first, followed by removal of positive impulses. The standard median filtered image with a 5 by 5 squared-shaped window is shown in Fig. 1(e). We conclude that the RAMF is superior to the nonlinear mean L_p filter [2] and the standard median filter in removing positive and negative impulse noises simultaneously.

III. SECOND NOISE MODEL: SAMF

A. Noise Model

In the second model, the noise corrupted pixel is $x_{ij} = s_{ij} + n_{ij}$ where n_{ij} is iid impulsive noise having Laplacian or Cauchy or a mixture of Gaussian and Cauchy distributions. This SAMF algorithm in this instance detects the width of the impulse and adjusts the window accordingly until the noise is eliminated.

B. Filter Structure

This filter for the second noise model is an extension and simplification of Lin's adaptive algorithm [5] in that it can handle a dense mixture of positive and negative impulses. It consists of two operations: detection followed by filtering.

Detection Operation: We define the test statistics for $j = 1 \rightarrow 3$

$$d_{+j} \triangleq x_{k+j-1} - x_{k+j} \text{ and } d_{-1} \triangleq x_k - y_{k-1} \tag{7}$$

where y_{k-1} is the median filter output at sample time $k-1$.

Stage 1: Detects impulse of size 1.

If $(d_{+1} > r_1$ and $d_{-1} > r_1)$ or $(d_{+1} < -r_1$ and $d_{-1} < -r_1)$

we declare one impulse present at location k and eliminate it by median filter of size 3. The program then shifts to the next pixel location $k+1$.

Stage 2: Detects impulses of size 2 if there is no impulse of size 1 in Stage 1.

If $(d_{+2} > r_2$ and $d_{-1} > r_2)$ or $(d_{+2} < -r_2$ and $d_{-1} < -r_2$

algorithm then declares two impulses present at locations k and $k+1$. It then eliminates these with two successive median filters of sizes 5 and 3, respectively, corresponding to pixel location k and $k+1$. Program then shifts to pixel at location $k+2$.

Stage 3: Detects impulses of size 3 if there is no impulse of size 2.

If $(d_{+3} > r_3$ and $d_{-1} > r_3$ or $(d_{+3} < -r_3$ and $d_{-1} < -r_3)$

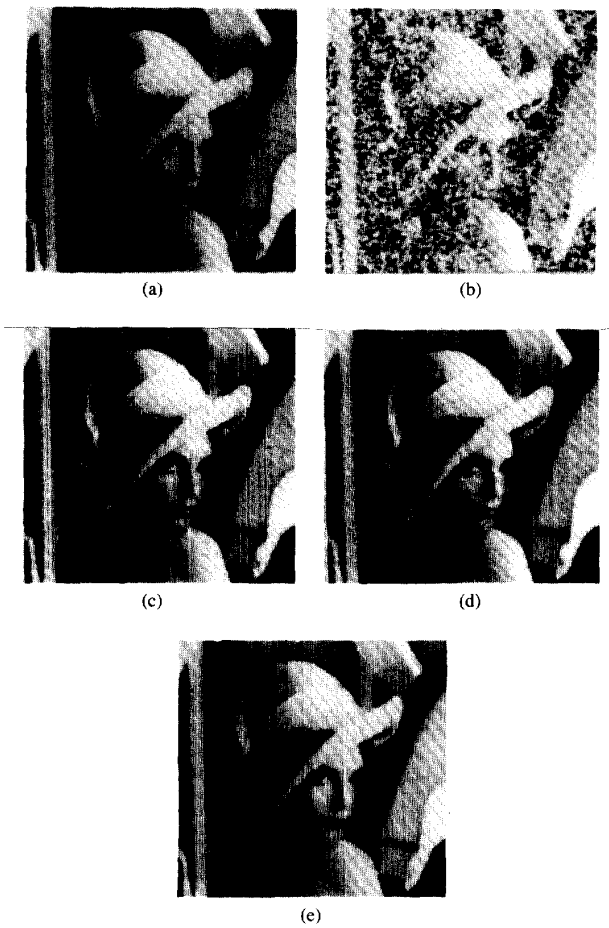

Fig. 1. (a) Original image; (b) noisy image ($p = 0.3$, $q_r = 0.5$). Outputs of filtering noisy image by (c) RAMF, (d) L_p filter [2], and (e) median filter.

the algorithm detects impulses at locations at k, $k+1$, $k+2$ and eliminates these with median filters of sizes 7, 5, and 3, replacing the corrupted pixel values by the median-filtered one. The program then shifts to the pixel location $k+3$.

Averaging Filter: If stages (1), (2), and (3) fail, we declare no impulse present at location k and call for simple averaging to reduce the Gaussian noise in the signal. In this case, the program then shifts to examine the pixel at location $k+1$. Note that impulse noise of size 4 will not be detected in this 3-stage algorithm. They will pass through attenuated only by the averaging filter. The maximum complexity of this configuration is set by the highest stage. In the 3-stage algorithm, on the order of (7 log 7 + 5 log 5 + 3 log 3) sorting operations are needed. The detectors are simple comparators. The looping is automatically terminated at the bottom of any particular stage.

Filtering Levels: The median filters are stacked depending on the size of the detected impulse. For example, if we detected an impulse of size 3 at stage 3, the top window is set equal to 7, and the algorithm proceeds as follows:

$$\text{level } 1: y_k^{(1)} = \text{med}\{x_{k-3}, \cdots, x_k, \cdots, x_{k+3}\}. \tag{8}$$

The center pixel is replaced by this median and inputted to the

$$\text{level } 2: y_{k+1}^{(2)} = \text{med}\{x_{k-1}, y_k^{(1)}, x_{k+1}, x_{k+2}, x_{k+3}\}. \tag{9}$$

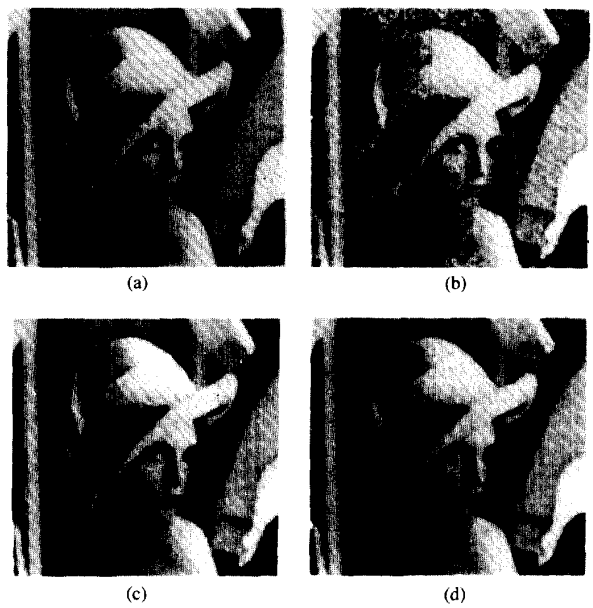

Fig. 2. (a) Original image; (b) noisy image ($\epsilon = 0.8$, $\sigma = 10$, $\lambda = 8$). Outputs of filtering noisy image by (c) SAMF and (d) Lin filter [5].

Then, for level 3, we use

$$\text{level } 3: y_{k+2}^{(3)} = \text{med}\{y_{k+1}^{(2)}, x_{k+2}, x_{k+3}\}. \tag{10}$$

If no impulse is detected, rather than do no filtering, we use a sample mean with censored data using x_k as the reference point. This output gives y_k as sample mean of $x_j \in L_\sigma$, where $L_\sigma = \{x_j | x_k - c \le x_j \le x_k + c, j \in (k-3, k+3)\}$, and c corresponds to a 3σ value.

2-D Version: For the 2–D algorithm with a cross-shaped window, we define the test statistics for $k = 1 \rightarrow 3$

$$\begin{aligned} d_{h+k} &\triangleq x_{i,j+k-1} - x_{i,j+k} \text{ and } d_{h-1} \triangleq x_{ij} - y_{i,j-1} \\ d_{v+k} &\triangleq x_{i+k-1,j} - x_{i+k,j} \text{ and } d_{v-1} \triangleq x_{ij} - y_{i-1,j}. \end{aligned} \tag{11}$$

Based on the 1–D algorithm, the window size is determined in both horizontal and vertical directions simultaneously. To reduce edge smearing in the diagonal directions, the window size decision for 45 and 135° directions are added.

C. Simulation Results

Fig. 2 compares the SAMF with Lin's adaptive filter [5]. The test image is the same as that shown in Fig. 1(a).

The noise consists of a mixture of two pdf's

$$f(x) = (1-\epsilon)g(x) + \epsilon h(x).$$

Here, $g(x)$ is $N(0, \sigma^2)$ and $h(x)$ is Cauchy with parameters λ. Fig. 2(b) shows the noise corrupted image with $\epsilon = 0.8$, $\sigma = 10$, and $\lambda = 8$. Fig. 2(c) and (d) shows, respectively, the SAMF filtered image and the Lin's filtered image. The thresholds τ_1, τ_2, and τ_3 will depend on σ, λ, and ϵ. These values were varied over the range $10 \rightarrow 35$ with no perceptible difference in performance. The values $\tau_1 = \tau_2 = \tau_3 = 15$ were found to provide a reasonable compromise between detection of an impulse and a false alarm. This test result shows that the SAMF performs better than the Lin's adaptive filter in removing a mixture of impulsive and nonimpulsive noises while preserving sharpness.

We conclude that the SAMF is superior to the median filter with adaptive length [5] in two respects: a) simpler and b) better performing.

IV. Concluding Remarks

Based on two types of impulse noise corrupted image models, we have introduced two new algorithms for adaptive median filter with variable window size for removal of high density impulse noises while preserving image sharpness: the *ranked-order based adaptive median filter* (RAMF) and the *impulse size based adaptive median filter* (SAMF).

The RAMF, based on a two-level test, is simple in its operation and removes positive and negative impulse noise simultaneously while preserving sharpness better than the nonlinear mean L_p filter [2].

The SAMF, based on impulse noise size detection inside a window, is simpler than Lin's adaptive scheme [5] and removes high density impulses, smoothes nonimpulsive noise, and preserves details better than Lin's scheme.

The simulation results also show that the performance of these filters are superior to that of the median filter.

References

[1] Y. H. Lee and S. A. Kassam, "Generalized median filtering and related nonlinear filtering techniques," *IEEE Trans. Acoust., Speech, Signal Processing*, vol. ASSP-33, pp. 672–683, June 1985.

[2] A. Kundu, S. K. Mitra, and P. P. Vaidyanathan, "Application of two-dimensional generalized mean filtering for removal of impulse noises from images," *IEEE Trans. Acoust., Speech, Signal Processing*, vol. ASSP-32, no. 3. pp. 600–609, June 1984.

[3] I. Pitas and A. N. Venetsanopoulos, "Nonlinear mean filters in image processing," *IEEE Trans. Acoust., Speech, Signal Processing*, vol. ASSP-34, no. 3, pp. 573–584, June 1986.

[4] Y. H. Lee and S. Tantaratana, "Decision-based order statistic filters," *IEEE Trans. Acoust., Speech, Signal Processing*, vol. 38, pp. 406–420, Mar. 1990.

[5] H. M. Lin and A. N. Wilson, Jr., "Median filters with adaptive length," *IEEE Trans. Circuits Syst.*, vol. 35, no. 6, June 1988.

[6] H. Hwang, "Multilevel adaptive nonlinear filters for edge detection and noise suppression," Ph.D. dissertation, Appendix C, Polytechnic Univ., June 1991.

High-Order Moment Computation of Gray-Level Images

Bingcheng Li

***Abstract*— This correspondence describes an efficient approach to calculate geometric moments of a 2-D gray-level image. It is shown both theoretically and experimentally that the new method compares favorably with previous techniques, especially for high-order moments.**

I. Introduction

Two-dimensional moments have been widely used in computer vision. Typical examples of applications involving lower order moments are pattern recognition [1], [2], [5], [6], [8], edge detection [4], orientation determination [3], [6], [7], and image normalization [3]. There have also been recent attempts to use high order geometric moments for image analysis [10], image reconstuction [11], [12], pattern recognition [13], and texture classification [21]. Although geometric moments have found wide applications, their computation still constitutes a challenge, especially for high orders.

Manuscript received April 21, 1992; revised January 25, 1994. The associate editor coordinating the review of this paper and approving it for publication was Dr. Michael Unser.

The author is with the University of Michigan-Dearborn, Dearborn, Michigan 48128 USA.

IEEE Log Number 9409273.

Several fast algorithms have been described for binary images [14]–[17]. Hatamian *et al.* proposed a IIR filtering-based approach to compute geometric moments for gray-level images. Their method uses no multiplications, and is well suited for low-order moment computations. However, when the moment order is high, it is difficult to derive the linear transform between the IIR filter output and the geometric moments. Furthermore, the computation of the transform as formulated by these authors is not necessarily the most efficient.

In this correspondence, we propose a new method to compute geometric moments of gray-level images. Instead of computing geometric moments directly, we first calculate auxiliary moments, which correspond to the inner product of the image and a linear combination of monomials. The geometric moments can then be computed by another linear transformation. For computational efficiency, the auxiliary moments are selected so that they correspond to the output of a IIR filter bank. In order to simplify the derivation of the linear transform, we introduce a new generating function that links the geometric moments with the IIR filter output. We then show that the linear transform B is the product of a series of $\phi-$matrices and that it can be implemented by a simple systolic structure. Finally, the new method is used to compute 2-D geometric moments, and a comparison with other techniques is provided.

II. Filtering-based Computation of Moments

In this section, we first prove that the inner product of two functions can be converted into a convolution. Then, a vector and matrix summation and their convolution are defined, and are used to simplify the computation of moments.

A. Inner Product and Scalar Convolution

The inner product of function $f(x)$ and $d(x)$ in [0, N] is defined as

$$<f, d>_N = \sum_{x=0}^{N} f(x)d(x). \tag{1}$$

Proposition 1: The inner product $<f, d>$ is the output at $x = N$ of a filter $d(x)$ with input $f(N - x)$, that is

$$\sum_{x=0}^{N} f(x)d(x) = d(x) * f(N - x)\,|_{x=N} \tag{2}$$

where * denotes the convolution.

The pth-order geometric moment is defined as

$$m_p = \sum_{x=0}^{N} x^p f(x). \tag{3}$$

From Proposition 1, we can convert (3) into

$$m_p = d(x) * f(N - x)\,|_{x=N} \tag{4}$$

where $d_p(x) = x^p$.